

# Madden-Julian Oscillation: Recent Evolution, Current Status and Predictions



Update prepared by: Adam Allgood  
Climate Prediction Center / NCEP  
19 November 2018

# Outline

Overview

Recent Evolution and Current Conditions

MJO Index Information

MJO Index Forecasts

MJO Composites

# Overview

- The MJO slowed down and weakened over the past few days, partly due to interference with both the base state and a strong equatorial Rossby wave over the West Pacific.
- Dynamical model MJO index forecasts depict continued robust MJO activity during the next two weeks. The GEFS forecasts indicate a high amplitude event crossing the Pacific during Week-1 and the Western Hemisphere during Week-2, while the ECMWF has a faster propagating and less amplified event. Statistical guidance also supports robust MJO activity.
- As the MJO enhanced phase crosses the Pacific, it will begin constructively interfering with the base state that is transitioning towards El Niño conditions.
- The MJO is likely to play a role in tropical-extratropical teleconnections over the next several weeks. A high amplitude Pacific MJO event tends to favor a transition to a negative NAO pattern and colder conditions over the eastern CONUS, which is fairly consistent with long range dynamical model forecasts.

Additional potential impacts across the global tropics and a discussion for the U.S. are available at:  
<http://www.cpc.ncep.noaa.gov/products/precip/CWlink/ghazards/index.php>

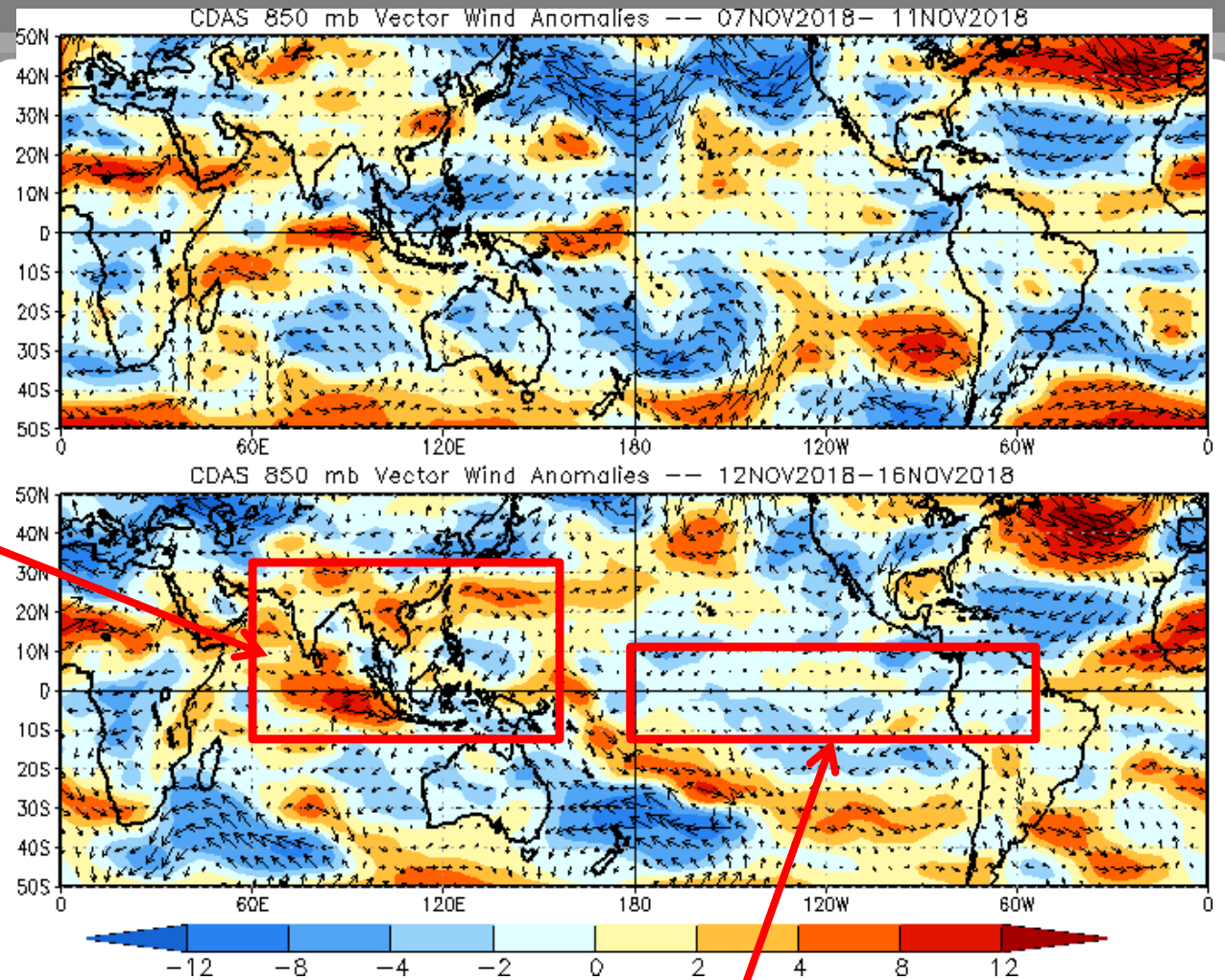
# 850-hPa Vector Wind Anomalies ( $\text{m s}^{-1}$ )

Note that shading denotes the zonal wind anomaly

**Blue shades:** Easterly anomalies

**Red shades:** Westerly anomalies

Westerlies persisted over the eastern Indian Ocean, while an anomalous anticyclonic gyre developed over the northern Maritime Continent.



The low level anomaly field was weak over the Pacific due to competing MJO and low frequency signals.

# 850-hPa Zonal Wind Anomalies ( $\text{m s}^{-1}$ )

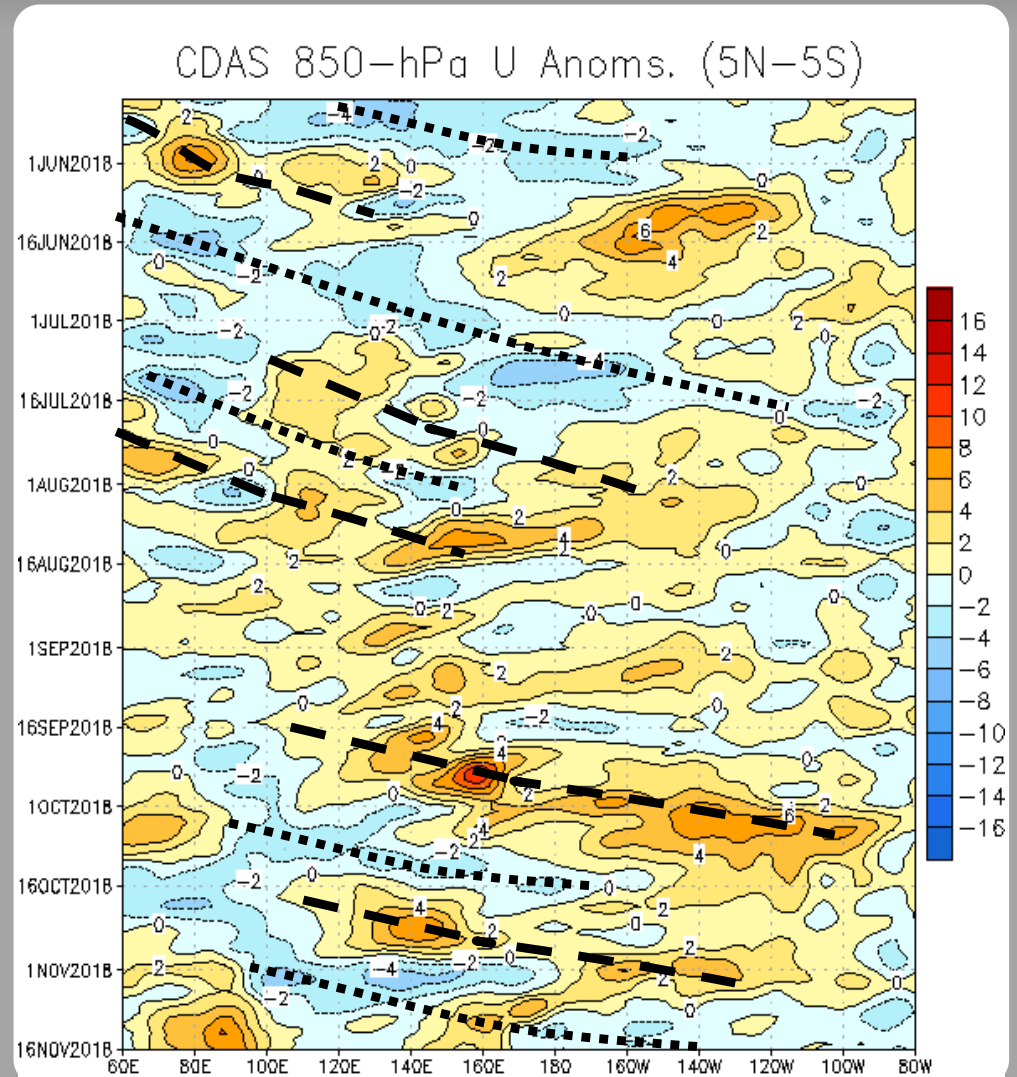
Westerly anomalies (orange/red shading) represent anomalous west-to-east flow

Easterly anomalies (blue shading) represent anomalous east-to-west flow

Westward moving variability weakened the MJO signal in June. A weak intraseasonal signal re-emerged during mid to late July.

From August through mid-September, other modes, including Rossby wave and tropical cyclone activity, influenced the pattern. Another rapidly propagating intraseasonal feature during late September generated robust westerly wind anomalies across the Pacific.

During late September and October, westerly anomalies increased in amplitude and duration over the equatorial Pacific, consistent with a gradual transition towards El Niño conditions. More recently, another robust MJO event interfered with the base state, while Rossby wave activity interfered with the MJO.



# OLR Anomalies - Past 30 days

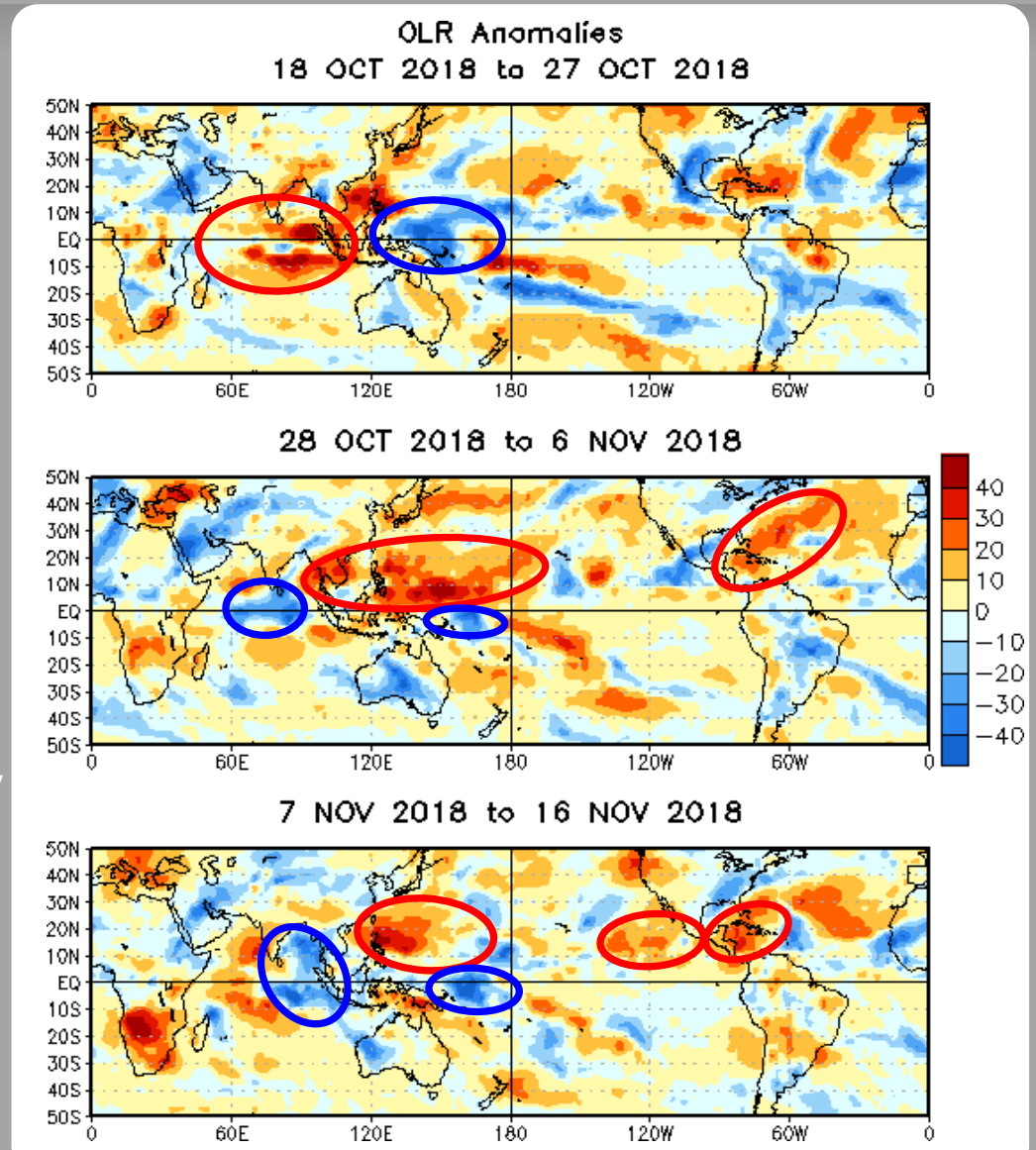
Drier-than-normal conditions, positive OLR anomalies (yellow/red shading)

Wetter-than-normal conditions, negative OLR anomalies (blue shading)

During late October, the suppressed phase of the MJO overspread the Indian Ocean. Constructive interference between the MJO and low frequency state resulted in enhanced convection across the equatorial West Pacific.

By early November, suppressed convection shifted eastward to the West Pacific. A signal rapidly returned to the Indian Ocean, resulting in a small area of enhanced convection. The western Atlantic quieted down as the later part of the hurricane season arrived.

Convection increased over the Indian Ocean by mid-November as the new MJO event strengthened. An area of enhanced convection persisted over the equatorial West Pacific, due in part to Rossby wave activity. Suppressed convection overspread the Western Hemisphere tropical cyclone basins, other than a single robust wave east of the Lesser Antilles.



# Outgoing Longwave Radiation (OLR) Anomalies (7.5°S - 7.5°N)

Drier-than-normal conditions, positive OLR anomalies (yellow/red shading)

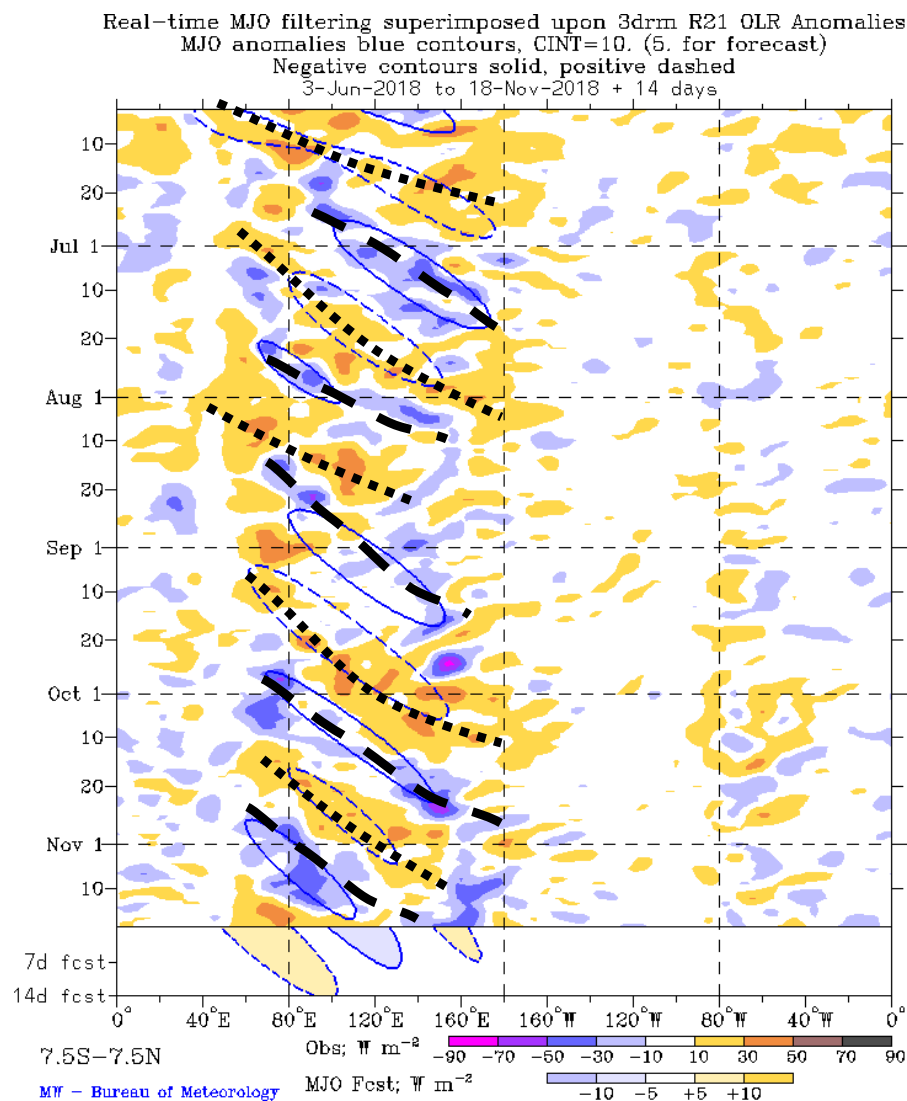
Wetter-than-normal conditions, negative OLR anomalies (blue shading)

The MJO became more active during July.

Kelvin waves, Rossby waves, and tropical cyclones dominated the pattern during August and early September, while the intraseasonal signal remained fairly weak.

During mid-September, the suppressed phase of the MJO emerged over the Eastern Indian Ocean and Maritime Continent. During early October, the suppressed signal propagated further east and enhanced convection emerged over the western Indian Ocean.

During November, the intraseasonal signal re-emerged over the Indian Ocean, and destructively interfered with the base state as the enhanced phase moved across the Maritime Continent. More recently, Rossby wave activity over the West Pacific interfered with the suppressed phase.



# 200-hPa Velocity Potential Anomalies (5°S - 5°N)

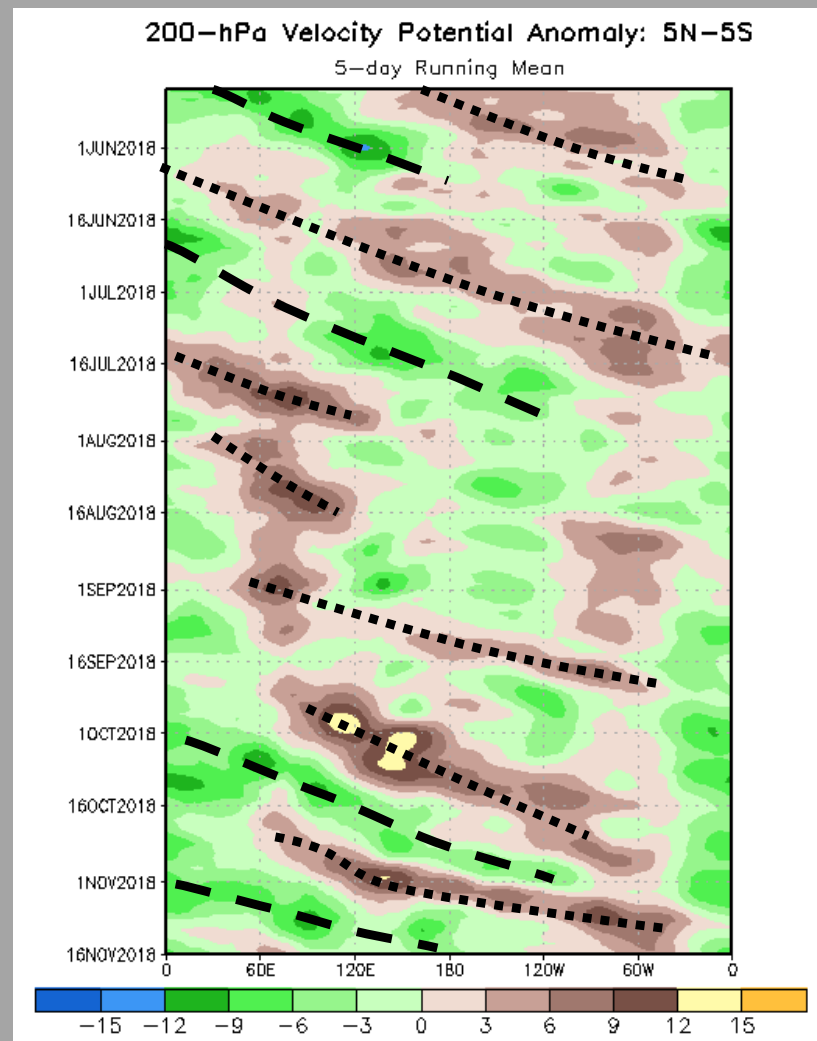
Positive anomalies (brown shading) indicate unfavorable conditions for precipitation

Negative anomalies (green shading) indicate favorable conditions for precipitation

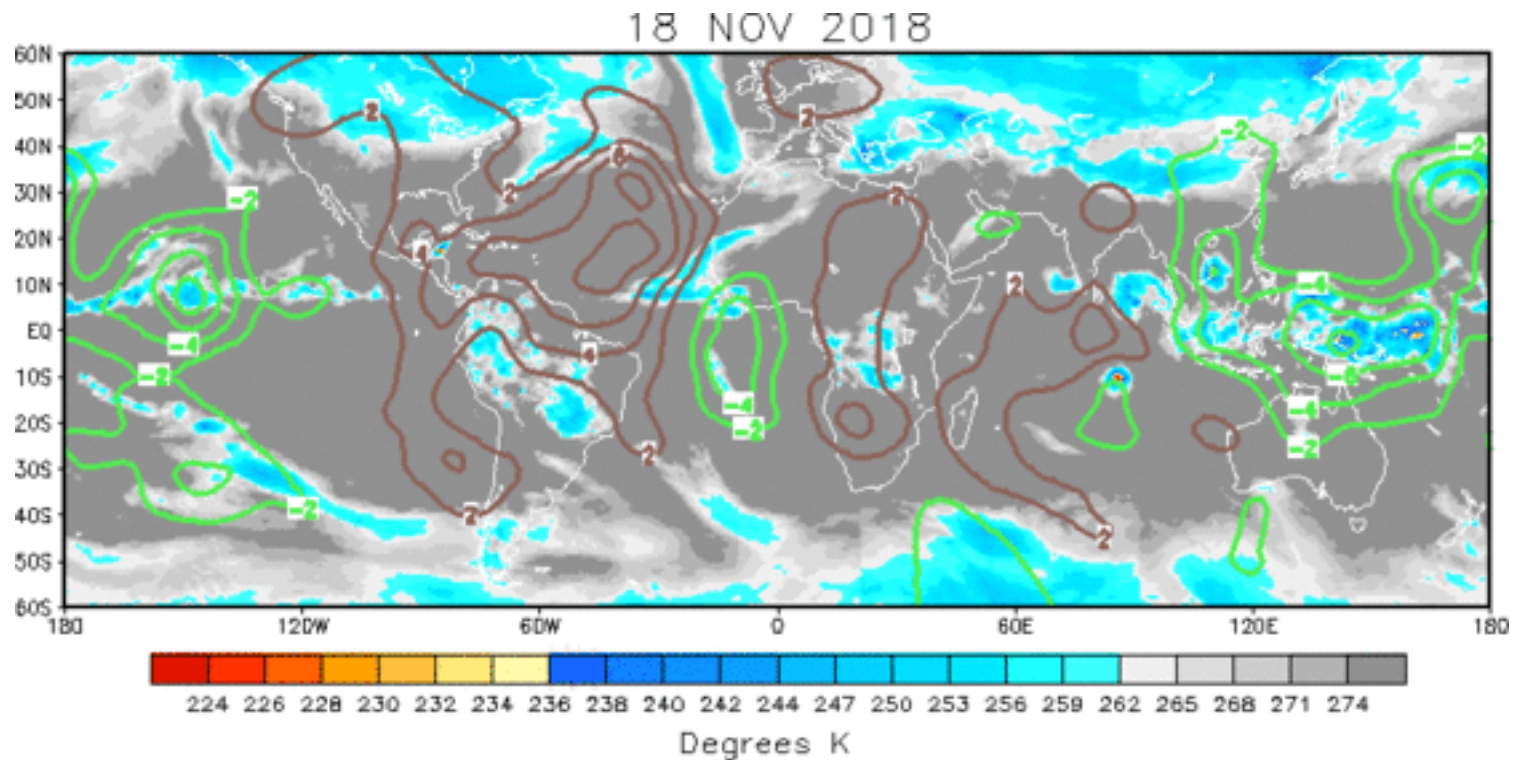
There was robust MJO activity through boreal spring along with the decay of La Niña conditions. The enhanced phase of the MJO weakened east of the Date Line during June. Eastward propagation of broad suppressed convection continued into early July. The upper-level footprint of the MJO re-emerged during mid-July, with a broad divergent signal propagating from the Maritime Continent to the central Pacific.

Starting in mid-July, a low-frequency dipole favoring enhanced (suppressed) convection over the east-central Pacific (Indian Ocean) emerged, consistent with a gradual transition towards El Niño conditions.

During mid-September, a robust intraseasonal signal constructively interfered with the base state over the Maritime Continent. The MJO signal persisted into October, and destructively interfered with the base state. More recently, renewed, fast-propagating MJO activity destructively interfered with the base state, with the enhanced signal beginning to re-emerge over the Pacific.



# IR Temperatures (K) / 200-hPa Velocity Potential Anomalies



The upper-level velocity potential pattern retains some coherency, with a broad enhanced (suppressed) envelope apparent over the Maritime Continent and Pacific (Western Hemisphere).

Positive anomalies (brown contours) indicate unfavorable conditions for precipitation

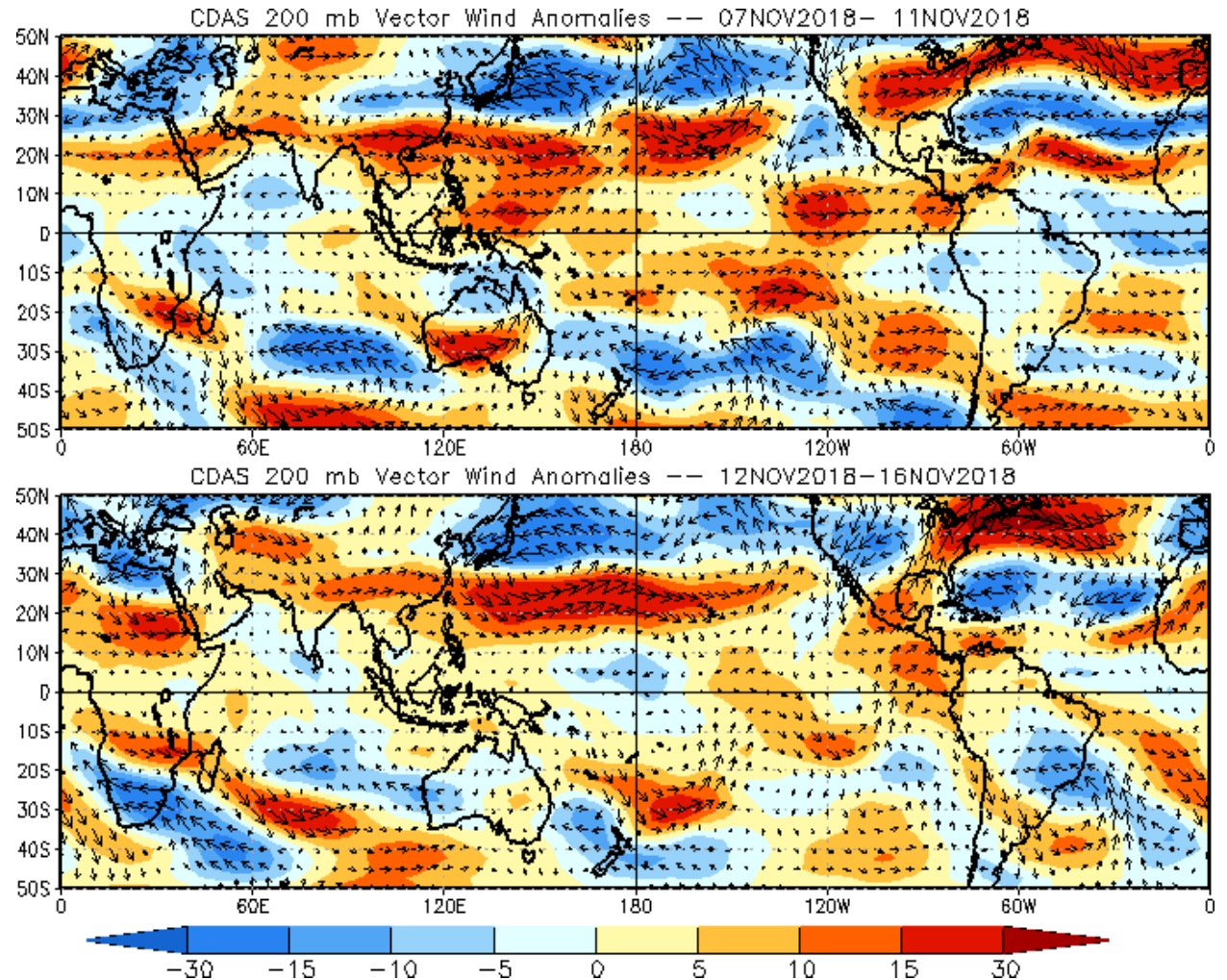
Negative anomalies (green contours) indicate favorable conditions for precipitation

# 200-hPa Vector Wind Anomalies ( $\text{m s}^{-1}$ )

Note that shading denotes the zonal wind anomaly

**Blue shades:** Easterly anomalies

**Red shades:** Westerly anomalies



Strong westerly anomalies  
extended across the North  
Pacific subtropics.

# 200-hPa Zonal Wind Anomalies ( $\text{m s}^{-1}$ )

Westerly anomalies (orange/red shading) represent anomalous west-to-east flow

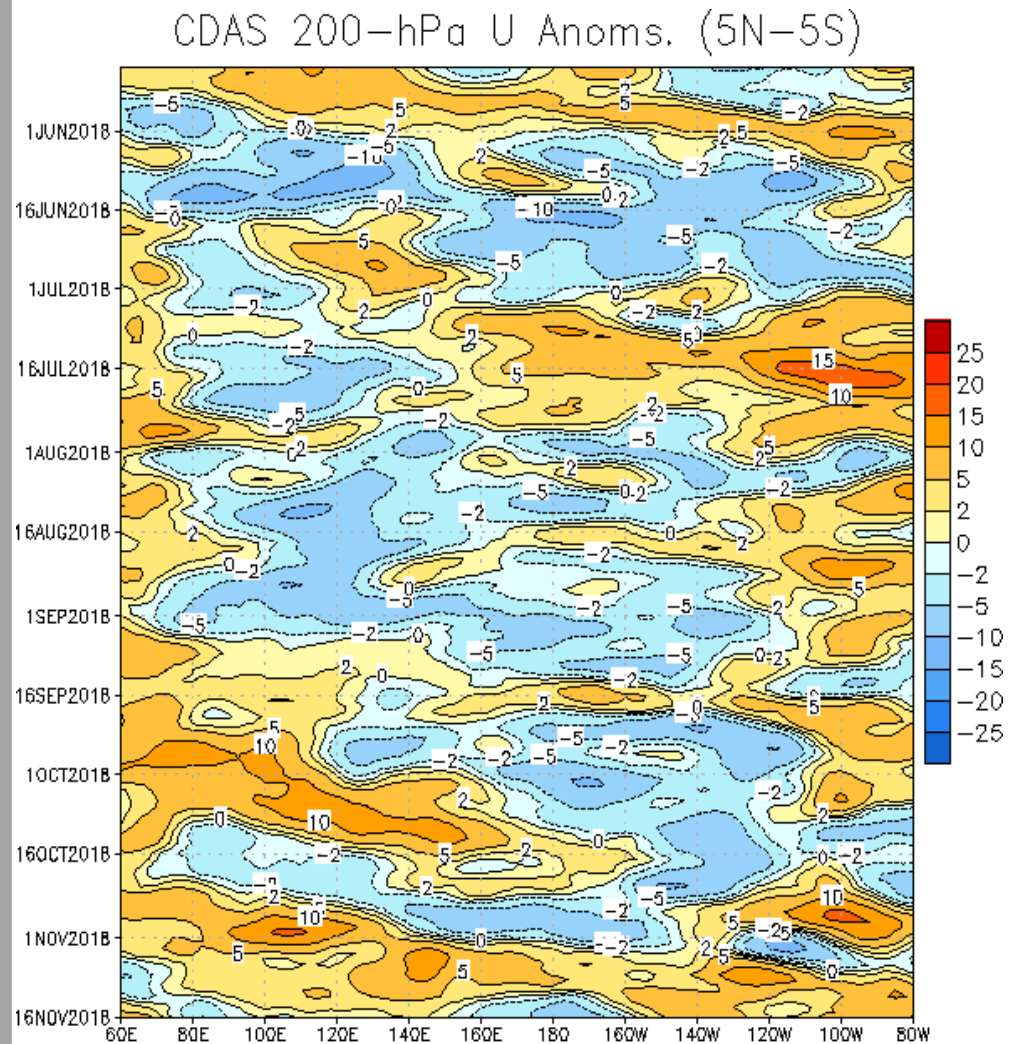
Easterly anomalies (blue shading) represent anomalous east-to-west flow

Weak westerly anomalies propagated eastward from the Indian Ocean to the Americas in early May; this pattern broke down in early June.

Anomalous westerlies amplified over the Maritime Continent in mid-June and propagated eastward at MJO-like phase speeds.

During August the intraseasonal pattern weakened, with Rossby wave activity influencing the West Pacific pattern.

Toward the end of October, anomalous westerlies strengthened over the Indian Ocean and since early November, have shifted east, persisting across the entire tropical Pacific. More recently, easterly anomalies returned to the central Pacific.



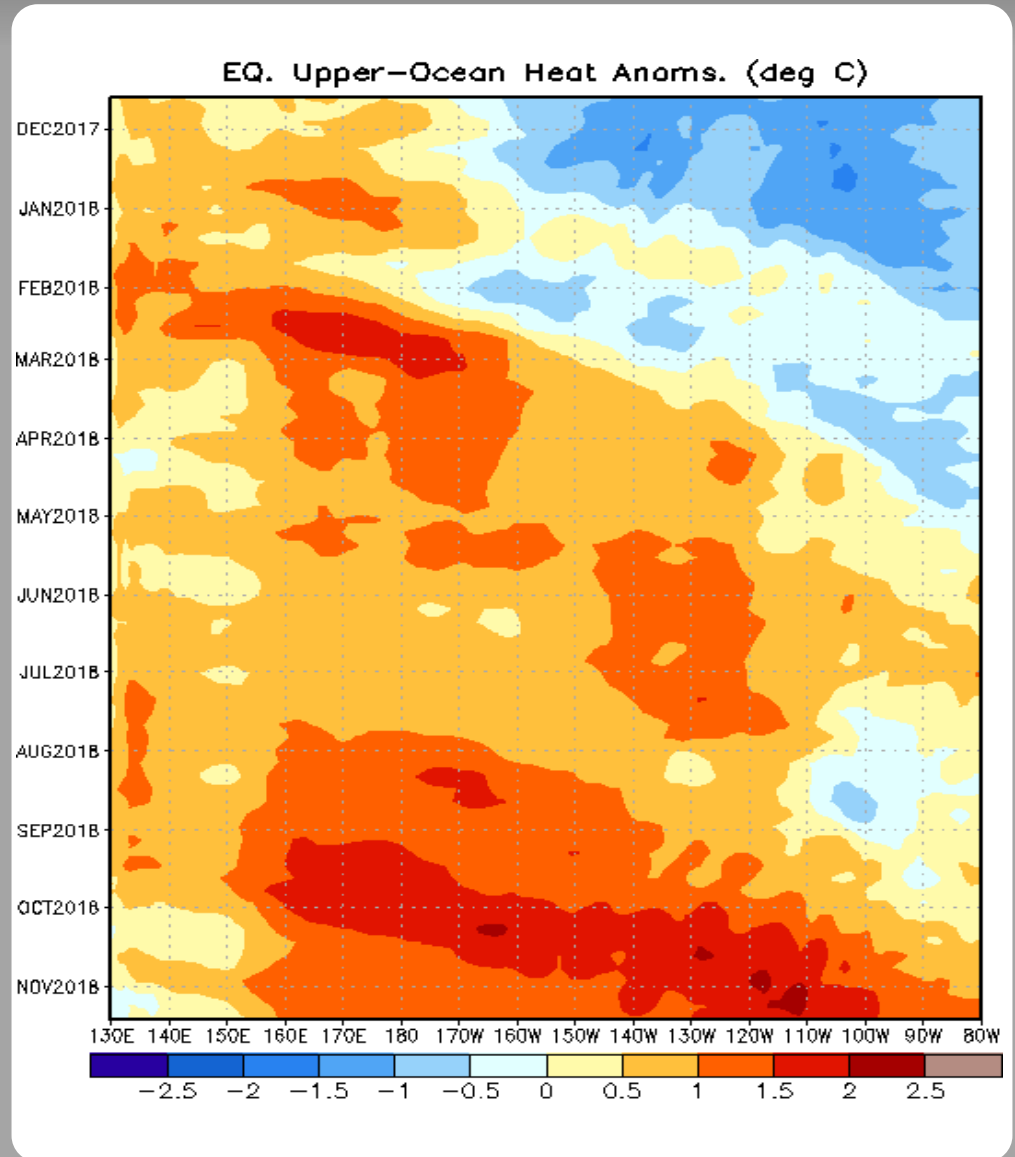
# Weekly Heat Content Evolution in the Equatorial Pacific

Oceanic Kelvin waves have alternating warm and cold phases. The warm phase is indicated by dashed lines. Downwelling and warming occur in the leading portion of a Kelvin wave, and upwelling and cooling occur in the trailing portion.

Negative upper-ocean heat content anomalies persisted in the central and eastern Pacific through December. A downwelling Kelvin wave associated with the intraseasonal signal weakened the negative anomalies across the east-central Pacific during late January and early February.

Several downwelling oceanic Kelvin waves contributed to the eastward expansion of relatively warm subsurface water during February. Positive anomalies have now been observed over most of the basin since April.

The westerly wind burst east of New Guinea in September triggered another oceanic Kelvin wave and round of downwelling, helping to reinforce the warm water availability for a potential El Niño event.



# MJO Index -- Information

The MJO index illustrated on the next several slides is the CPC version of the Wheeler and Hendon index (2004, hereafter WH2004).

Wheeler M. and H. Hendon, 2004: An All-Season Real-Time Multivariate MJO Index: Development of an Index for Monitoring and Prediction, *Monthly Weather Review*, 132, 1917-1932.

The methodology is very similar to that described in WH2004 but does not include the linear removal of ENSO variability associated with a sea surface temperature index. The methodology is consistent with that outlined by the U.S. CLIVAR MJO Working Group.

Gottschalck et al. 2010: A Framework for Assessing Operational Madden-Julian Oscillation Forecasts: A CLIVAR MJO Working Group Project, *Bull. Amer. Met. Soc.*, 91, 1247-1258.

The index is based on a combined Empirical Orthogonal Function (EOF) analysis using fields of near-equatorially-averaged 850-hPa and 200-hPa zonal wind and outgoing longwave radiation (OLR).

# MJO Index - Recent Evolution

The axes (RMM1 and RMM2) represent daily values of the principal components from the two leading modes

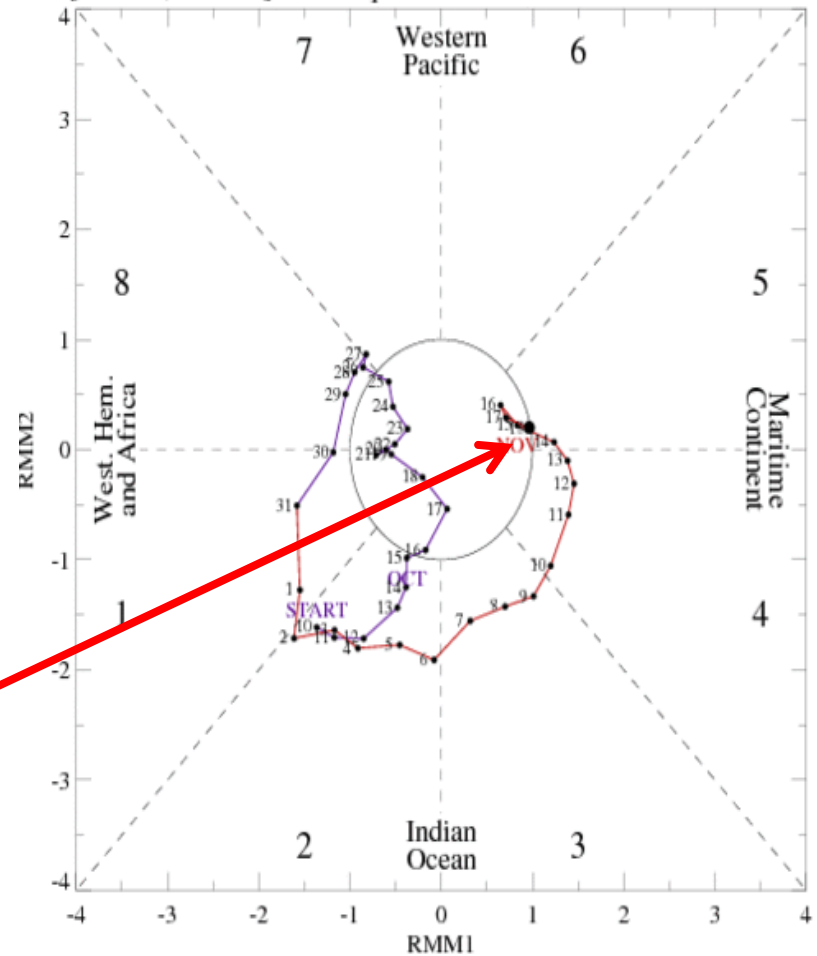
The triangular areas indicate the location of the enhanced phase of the MJO

Counter-clockwise motion is indicative of eastward propagation. Large dot most recent observation.

Distance from the origin is proportional to MJO strength

Line colors distinguish different months

[RMM1, RMM2] Phase Space for 10-Oct-2018 to 18-Nov-2018

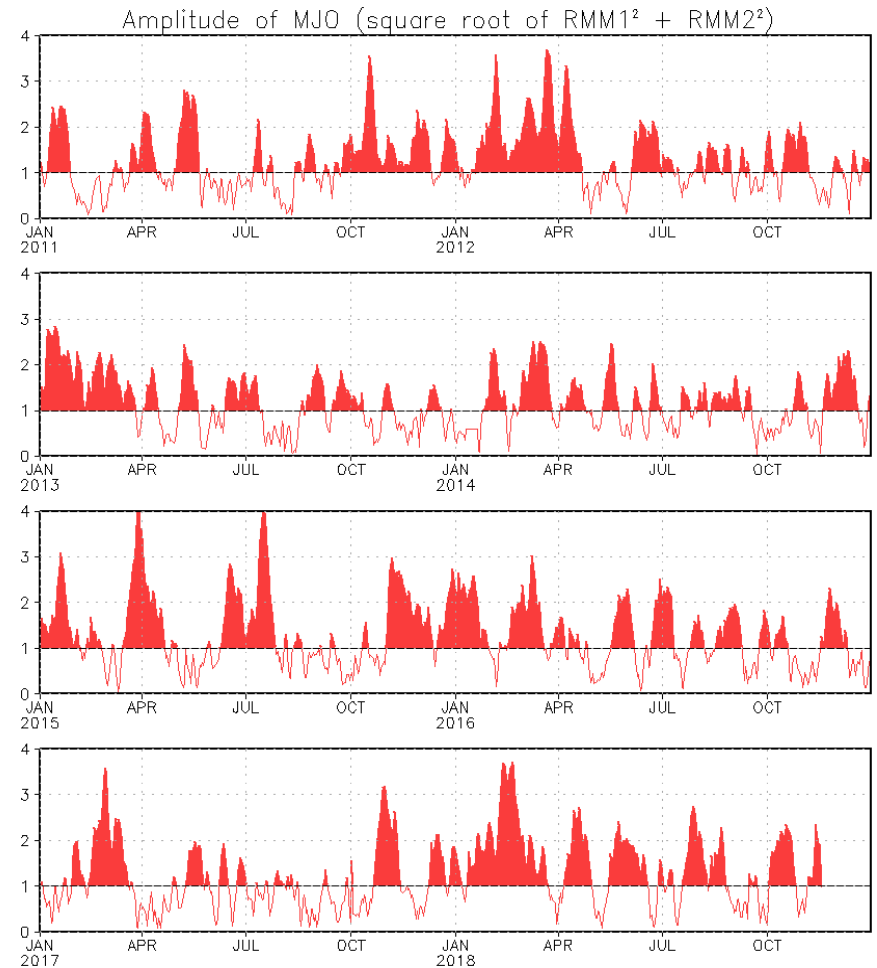


The RMM-based MJO index weakened during the past few days, possibly due to interference from a Rossby wave over the western Pacific.

# MJO Index - Historical Daily Time Series

Time series of daily MJO index amplitude for the last few years.

Plot puts current MJO activity in recent historical context.



# GFS Ensemble (GEFS) MJO Forecast

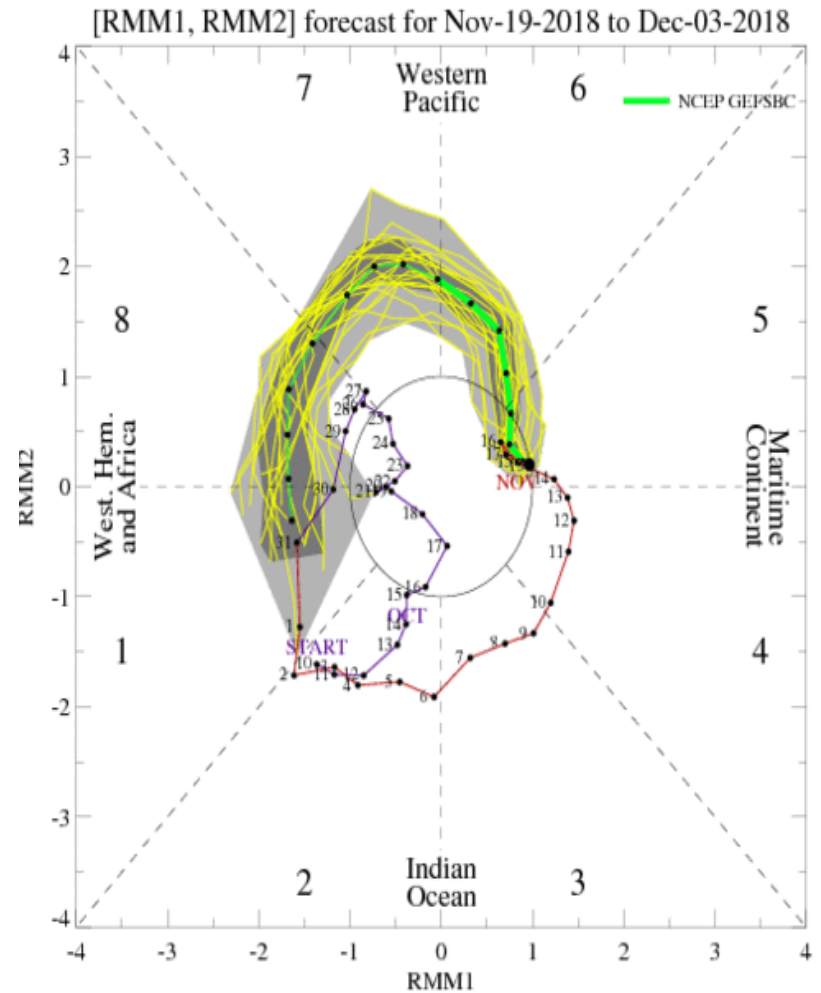
RMM1 and RMM2 values for the most recent 40 days and forecasts from the GFS ensemble system (GEFS) for the next 15 days

light gray shading: 90% of forecasts

dark gray shading: 50% of forecasts

The GEFS-based RMM-index forecast depicts robust MJO activity propagating across the Pacific to the Western Hemisphere during the next two weeks.

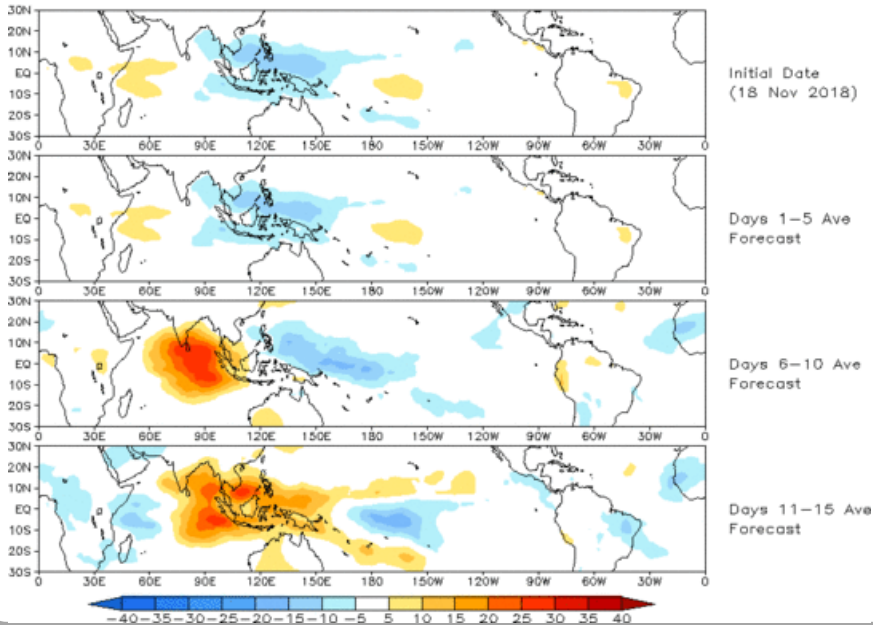
Yellow Lines - 20 Individual Members  
Green Line - Ensemble Mean



# Ensemble GFS (GEFS) MJO Forecast

Spatial map of OLR anomalies for the next 15 days

Prediction of MJO-related anomalies using GEFS operational forecast  
Initial date: 18 Nov 2018  
OLR

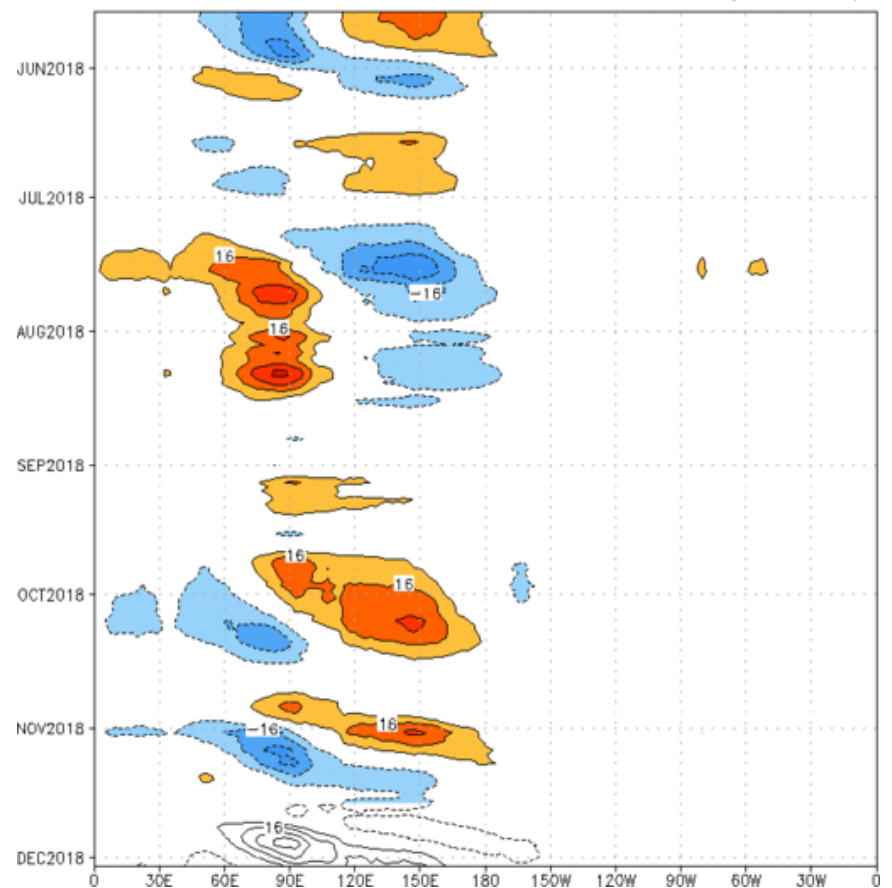


The GEFS RMM-based OLR forecast shows high-amplitude anomalies consistent with a robust MJO event.

Figures below show MJO associated OLR anomalies only (reconstructed from RMM1 and RMM2) and do not include contributions from other modes (*i.e.*, ENSO, monsoons, etc.)

Time-longitude section of (7.5° S-7.5° N) OLR anomalies - last 180 days and for the next 15 days

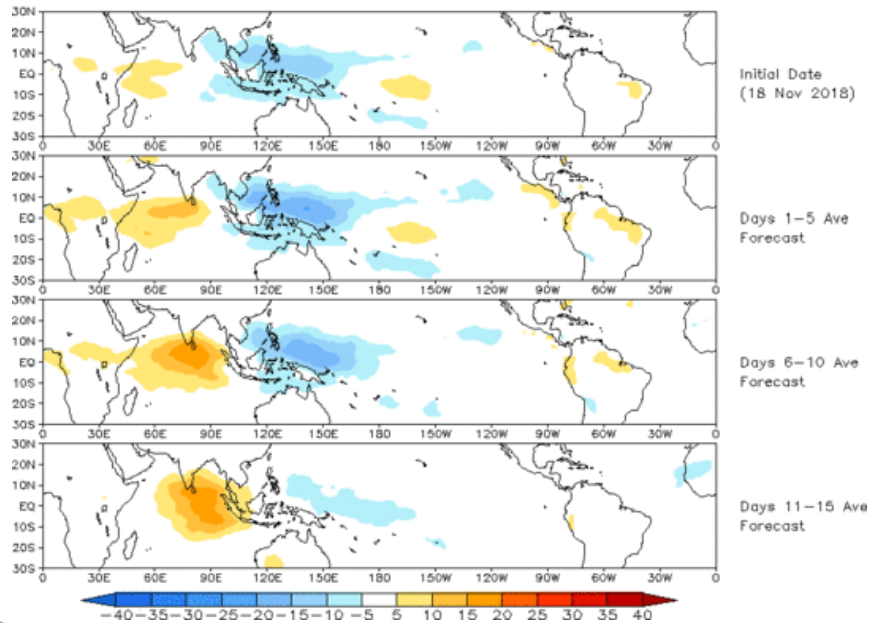
Reconstructed anomaly field associated with the MJO using RMM1 & RMM2  
OLR [7.5°S,7.5°N] (cont:4Wm<sup>-2</sup>) Period:19-May-2018 to 18-Nov-2018  
The unfilled contours are GEFS forecast reconstructed anomaly for 15 days



# Constructed Analog (CA) MJO Forecast

Spatial map of OLR anomalies for the next 15 days

OLR prediction of MJO-related anomalies using CA model reconstruction by RMM1 & RMM2 (18 Nov 2018)

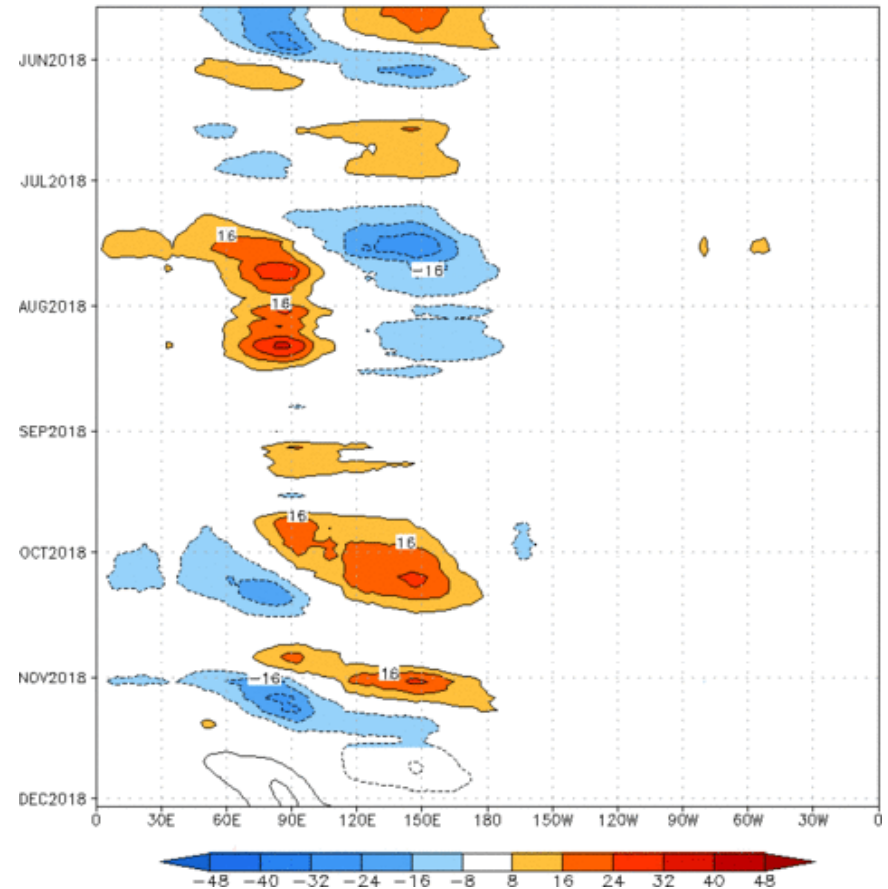


The OLR forecast based on the constructed analog RMM-index forecasts also depicts robust MJO activity with a slower phase speed than the GEFS.

Figures below show MJO associated OLR anomalies only (reconstructed from RMM1 and RMM2) and do not include contributions from other modes (*i.e.*, ENSO, monsoons, etc.)

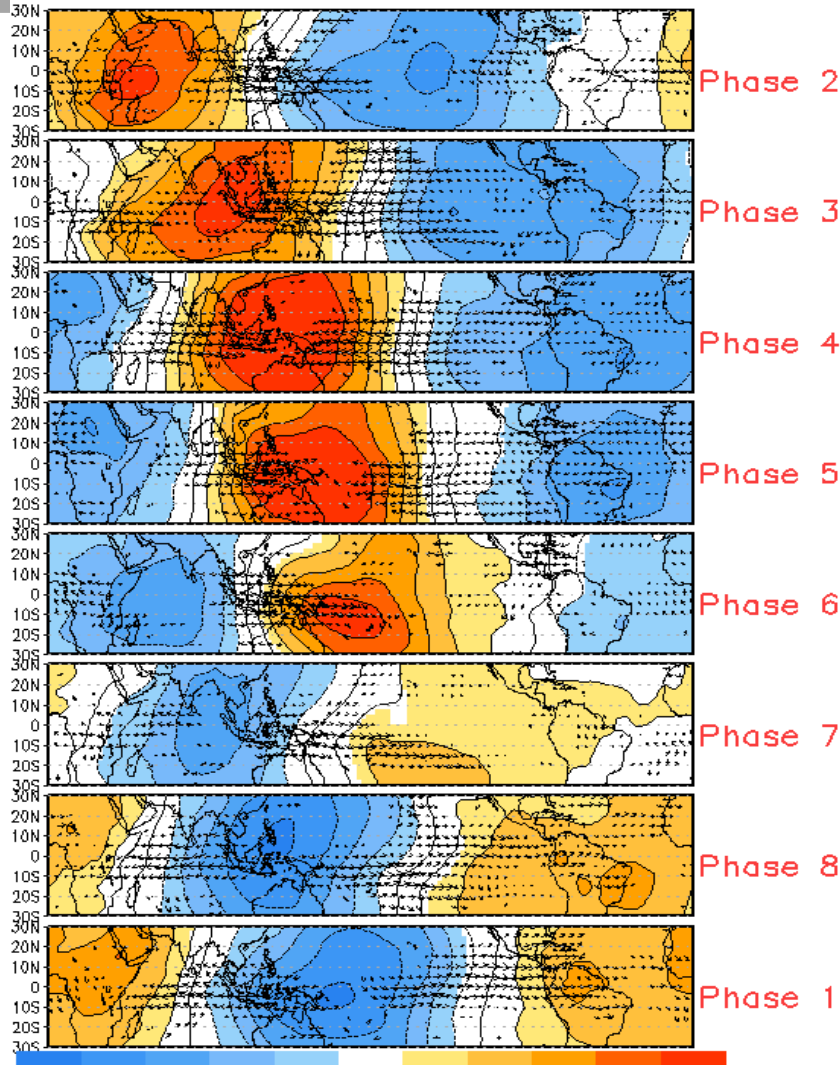
Time-longitude section of (7.5° S-7.5° N) OLR anomalies - last 180 days and for the next 15 days

Reconstructed anomaly field associated with the MJO using RMM1 & RMM2 OLR [7.5°S,7.5°N] (cont:4Wm<sup>-2</sup>) Period:19-May-2018 to 18-Nov-2018  
The unfilled contours are CA forecast reconstructed anomaly for 15 days

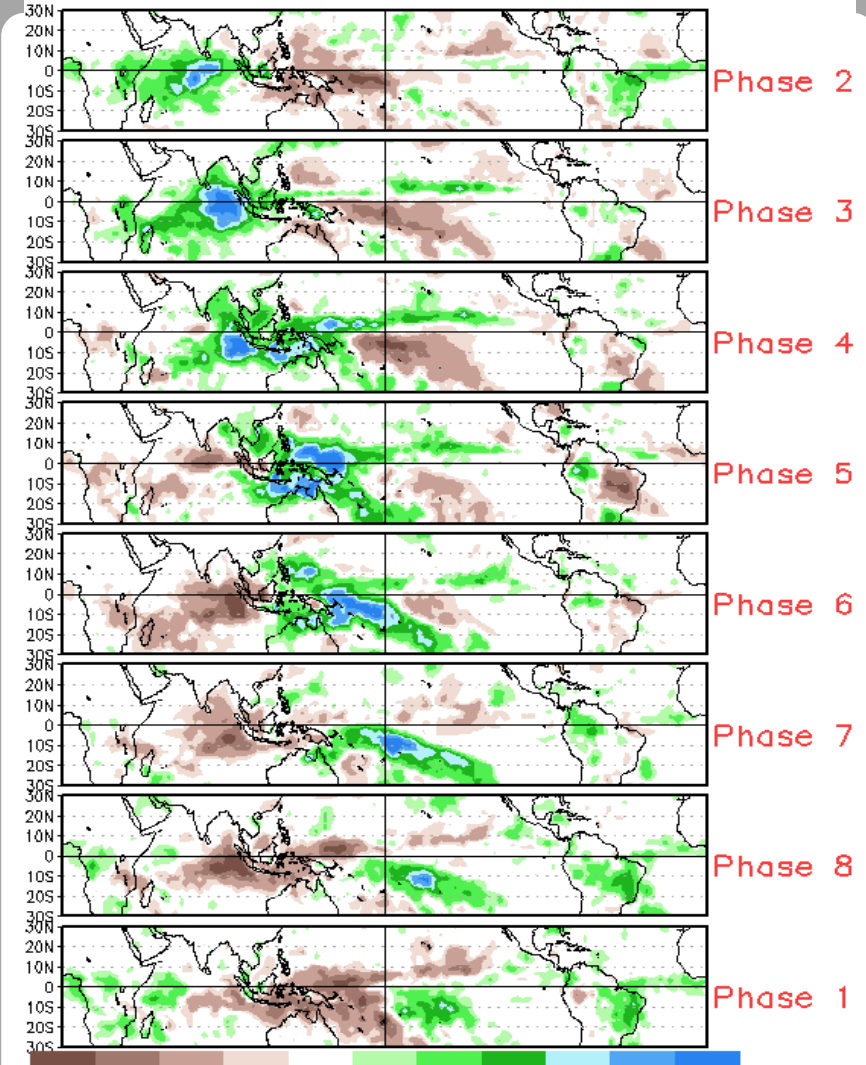


# MJO Composites - Global Tropics

850-hPa Velocity Potential and  
Wind Anomalies (Nov - Mar)



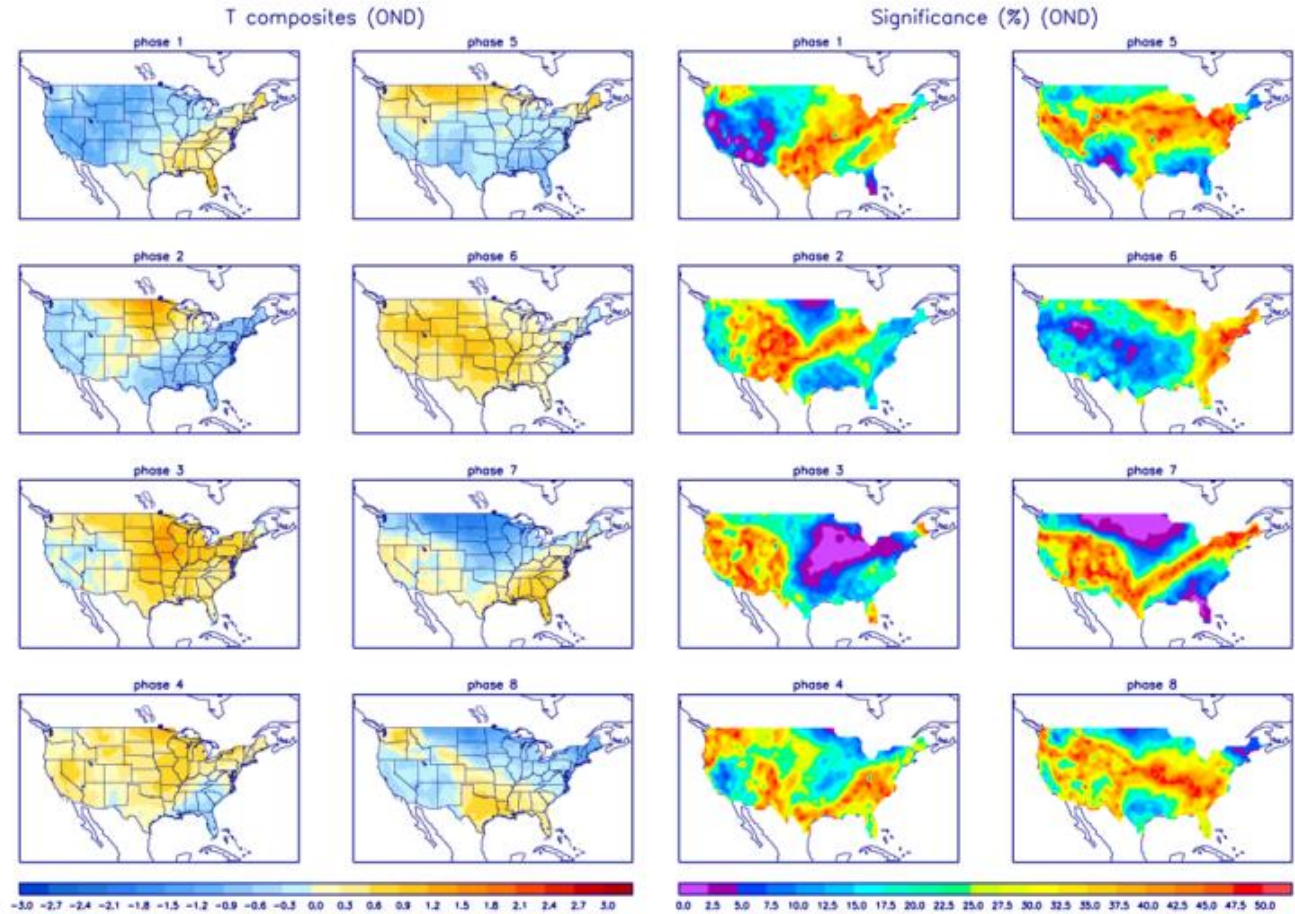
Precipitation Anomalies (Nov - Mar)



# U.S. MJO Composites - Temperature

Left hand side plots show temperature anomalies by MJO phase for MJO events that have occurred over the three month period in the historical record. Blue (orange) shades show negative (positive) anomalies respectively.

Right hand side plots show a measure of significance for the left hand side anomalies. Purple shades indicate areas in which the anomalies are significant at the 95% or better confidence level.



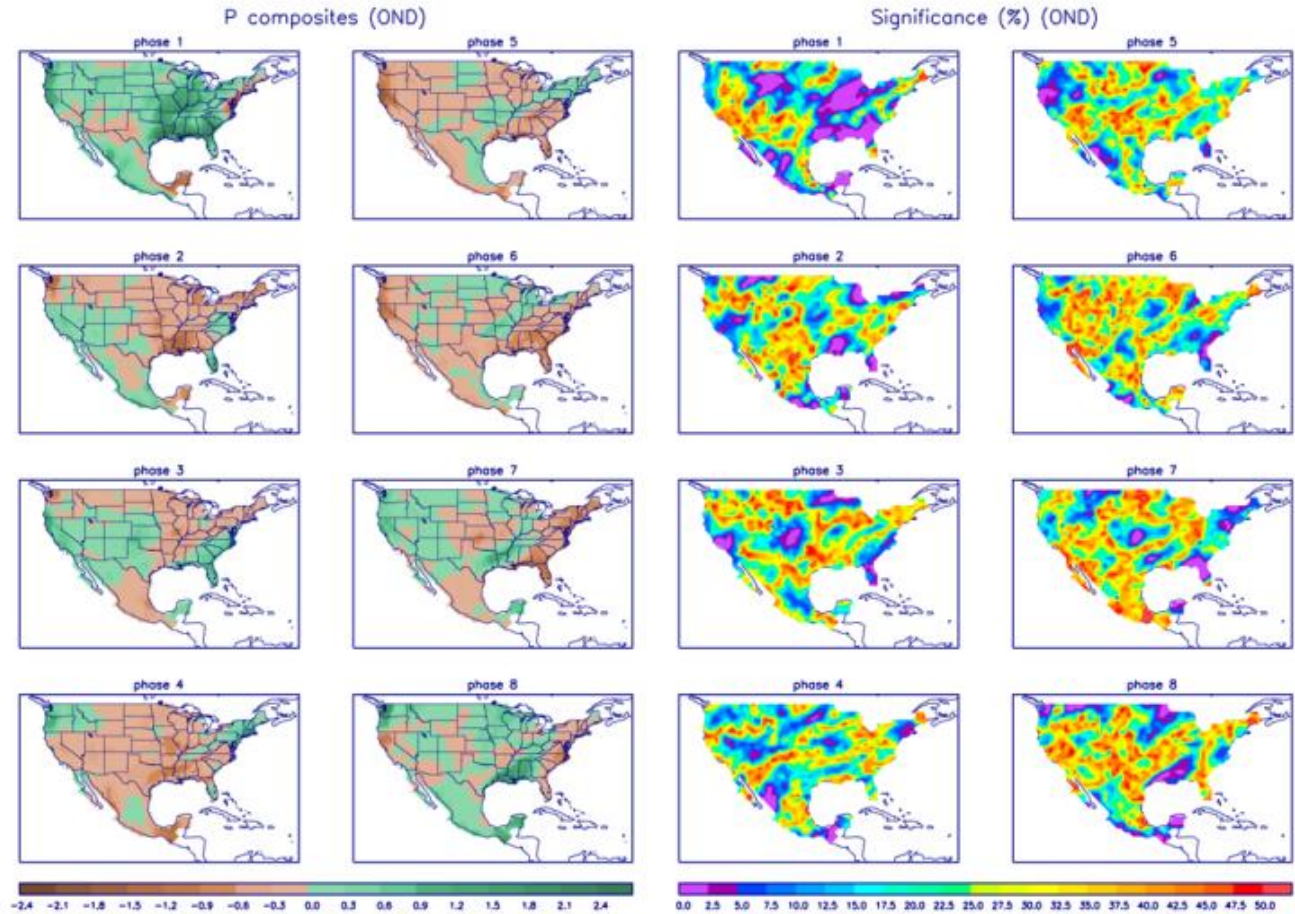
Zhou et al. (2011): A composite study of the MJO influence on the surface air temperature and precipitation over the Continental United States, *Climate Dynamics*, 1-13, doi: 10.1007/s00382-011-1001-9

<http://www.cpc.ncep.noaa.gov/products/precip/CWlink/MJO/mjo.shtml>

# U.S. MJO Composites - Precipitation

Left hand side plots show precipitation anomalies by MJO phase for MJO events that have occurred over the three month period in the historical record. Brown (green) shades show negative (positive) anomalies respectively.

Right hand side plots show a measure of significance for the left hand side anomalies. Purple shades indicate areas in which the anomalies are significant at the 95% or better confidence level.



Zhou et al. (2011): A composite study of the MJO influence on the surface air temperature and precipitation over the Continental United States, *Climate Dynamics*, 1-13, doi: 10.1007/s00382-011-1001-9

<http://www.cpc.ncep.noaa.gov/products/precip/CWlink/MJO/mjo.shtml>